08

Advanced Optical Metrology

Geoscience II

OLYMPUS

WILEY

Contents

Imprint

© Wiley-VCH GmbH
Boschstr. 12,
69469 Weinheim, Germany
Email: info@wiley-vch.de
Editor-in-Chief: Dr. Christina Poggel

Cover image: Becky Swora - Adobe-Stock.com | Olympus

Introduction

Geoscience includes all the natural sciences related to the structure, morphology, evolution, and dynamics of the Earth. Among them, geology deals with the origin, formation, and evolution of Earth, including its component materials and their structure. For geologists, grains and sediment are important since their study and analysis represent a powerful tool in classifying rocks or for describing a site's geomorphic setting. Characterizing the physical properties of grains, for example, is critical to determine the suitability of sediment for various uses or in the study of its geologic history. The main physical properties of grains are their size and size distribution, color, shape, and composition.

A basic tool for geoscientists is the optical microscope, which enables the magnification of sample images for analysis and careful inspection. The Olympus DSX1000 digital microscope is ideal for this application due to its large collection of easily interchangeable lenses, six observation methods available at the push of a button, fast macro to micro viewing, and accurate measurements thanks to a telecentric optical system.

Geoscientists study many types of sediments, including grains in a wide range of sizes and shapes. For example, gravel-sized particles have a nominal diameter of 2 mm, sand-sized particles have diameters ranging from ca. 2 mm to 62.5 µm, and clay is composed of particles having diameters less than 2 µm.[1] On the other hand, sands, for example, are usually composed of grains/units having different sizes and shapes, as shown in Figure 1. The wide range of sizes necessitates working with several magnifications and objectives with a range of working distances. Smaller samples require higher magnifications and objectives with shorter working distances. With conventional digital microscopes, this can be challenging since the objective can crash into the sample, potentially damaging it. This problem is solved with the DSX1000 digital microscope since its long working distance objectives enable the observation of uneven samples. These objectives are convenient for 3D samples since they combine the resolution of standard objectives with very long working distances, keeping the grains far from the optic to reduce the risk of damage.

Two important physical parameters of geological samples are their color and texture since they can be critical in the identification of the different minerals that compose the sample. Darkfield microscopy is the preferred method for imaging natural colors. On the other hand, accurate identification of texture requires a detailed observation of surface details, which necessitates illuminating the sample from above. The DSX1000 digital microscope can simultaneously work in brightfield and darkfield illumination methods from different directions. This feature, called MIX illumination,

Saint Vincent Paradise Beach, Caribbean Sea, Saint Vincent
Mineral sand with volcanic minerals
Field of view: 2.5 mm

makes the DSX1000 digital microscope ideal for the observation of geological samples.

Another important advantage the microscope offers to geoscience is its ability to acquire Z-stacks (focus stacking), which is a technique to combine images taken at different focus distances. The result is an image with a greater depth of field than any of the individual images. This is of particular interest for samples that have rough surfaces or with marked reliefs, like rocks or sediments.

For geoscientists, the DSX1000 digital microscope is a powerful tool for inspection geological sample. It combines low-magnification and high-magnification systems, offering a wide-magnification range in a single easy-to-use instrument. Moreover, the microscope possesses high-resolution, long working distance objectives that facilitate the capture of high-resolution, high-magnification images, enabling the inspection of fine details in the geological samples. In addition, the long working distance objectives provide ample space between the lens and sample to make observations without risking the optics. And with six observation methods available at all magnifications by simply pushing a button, the DSX1000 digital microscope offers geoscientists tremendous flexibility.

REFERENCES

[1] *Wentworth, C. K. A Scale of Grade and Class Terms for Clastic Sediments. J. Geol. 30, 377–392 (1922).*

[2] *Rebecca Chandler. Discovering the Unseen Beauty of Sand Under a Digital Microscope. https://www.olympus-ims.com/en/insight/discovering-the-unseen-beauty-of-sand-under-a-digital-microscope/ (2021).*

What you can also find in this eBook
Another recent research article on the application of portable X-Ray fluorescence spectroscopy for soil analysis. Learn more about how this method was used to scan soils of three agricultural fields in New Mexico after the Gold King Mine spill on **page 14** of this eBook.

You can find more exciting Geoscience articles in part 7 of our Advanced Optical Metrology eBook series.

01 The Unseen Beauty of Sand Under a Digital Microscope

© Becky Swora - Adobe-Stock.com

Annegret Janovsky is a senior specialist for industrial microscopy at Olympus who uses her imaging expertise for a unique hobby: microscopic sand photography. In her spare time, she collects sands from beaches around the world to produce beautiful, detailed images of their grains using our DSX1000 digital microscope.

In the following pages of this eBook, you will find eleven selected images from the more than three hundred that the cristallographer and her friends and family have collected over the years; we talked to Annegret about her favorite ones.

Was there any particular time you got interested in looking at sand?

Annegret: In 2015, I remembered sand I saw 25 years ago on my first travel with my future husband. And there was such a lovely lake in Scotland, it was called Loch Achilty. But back then we did not know the name of that lake. And at its bank, we found a sand I had never seen before. It was so crazy because it was not such a bright sand such as from the Mediterranean Sea or the Baltic Sea. Also, it was violet. I was so fascinated by this sand, but in those days, I never thought about collecting it or imaging it.

Later, when we got the first digital microscopes at Olympus, I was looking for good samples to see the quality of the images. I remembered this sand, but it took a while before I was able to collect any. We had to go back to Scotland to look for this lake. But there was no help on the Internet; nobody knew anything about this lake with violet sand. However, after two days, we were lucky and found this special sand again. And yes, after collecting a small amount of violet sand, I was interested in its composition, so I had a look using a DSX1000 digital microscope, and it was very interesting.

This was the beginning of my sand collection.

That is a nice way of getting into a new field of imaging and a new hobby at the same time. Since then, have you been collecting different types of sand on different holidays and travels?

Annegret: Yes, of course. But my colleagues, family, and friends all know of my hobby, so they collect sand for me when they travel. Currently, I have a collection of over 300 sands. Sometimes they are very similar to other sands I already have, but most of the sands are very interesting. Within almost every new sand is a new world.

The images in this eBook are only a sample of everything you have. Can you tell us more about the image of the violet sand on page 6?

Annegret: Yes, this is my very first sand, the one I mentioned before from Loch Achilty. On the large image at the bottom, you can see a macro photo of the lake. This is a pure mineral sand. It is violet, and, of course, has bright or natural colored grains. But there is also a range of dark grains included.

X-ray diffractometry analysis performed by one of my Olympus colleagues using our TERRA™ pXRD instrument have shown that the purple sand grains are garnets.

Loch Achilty, Scotland, UK
Mineral sand
Field of view: 3.2 mm

Star Sand, Taketomi Island, East China Sea, Japan
Biogenic sand made of forams
Field of view: 14 mm

The next image on page 7 is very interesting. What is the secret behind the shape of this sand?

Annegret: My two most important sands are the purple one we just discussed, as it was my first sand, and this sand, which is from Taketomi, a Japanese island in the East China Sea. It is so impressive—can you see the stars? This is organic sand, and it is composed of the shells of foraminifera—microscopic organisms that form hard shells of various shapes. These grains are particularly amazing as the whole shell is formed by a single-celled organism.

This is fascinating. How big are these grains?

Annegret: The foraminifera are relatively large at 2–3 mm each, so this image was taken using a 3x XLOB objective from Olympus. These objectives are useful for 3D samples because they combine the resolution of standard material objectives with very long working distances, reducing the risk of sand grains hitting the optics!

Toronto Islands,
Lake Ontario, Canada
Heavy mineral sand with pink and red garnets, black magnetite
Field of view: 2 mm

The next image that is really impressive is the one on page 8. What is the story behind that one?

Annegret: This is a sand that was collected by my daughter. It is from Lake Ontario near Toronto, Canada. In the large image you can see the photo of the beach with this reddish and black material. The reddish grains are garnets and the black ones are magnetite. It is a typical heavy mineral sand. Due to their weight, heavy minerals like garnet or magnetite can be accumulated on beaches, with lighter minerals being carried away by wind or by water.

This sand was imaged using a 10x XLOB objective. As with the first image, these grains are small and have interesting colors. From my experience of imaging different materials, I knew that darkfield microscopy is best for imaging natural colors. It is also useful to have a light source above the sample to capture surface details. The DSX1000 allows simultaneous brightfield and darkfield illumination from different directions, which is ideal for these types of samples. In fact, all of the images featured here were taken using MIX illumination.

Another fascinating image is the one shown on page 9. Where did you find this sand?

Annegret: This is sand from Lahinch in Ireland, and it’s completely different from the heavy mineral sand in the last photo from Lake Ontario and from the sand from Loch Achilty, as it is composed of biogenic components. Therefore, it is not possible to find out the origin of all the broken bits and pieces you can see in the image. They could be shells, foraminifera, or other organic materials; I don't know. But you can see a glassy, Y-shaped piece in the center of the image; this is a sponge spicule. And in the left bottom corner, there is another interesting shape. It is a fragment of a sea urchin spine.

A crucial advantage to using the DSX1000 digital microscope for imaging sand is its ability to acquire Z-stacks—all of the images here were acquired using focus stacking.

Figure 1: Organic sand collected from Lahinch in Ireland. This sand is composed of units having several sizes and shapes, forming a heterogeneous mix of purely biogenic components.[2]

Lahinch, Atlantic Ocean, Ireland
Biogenic sand with a Y-shaped sponge spicule, sea urchin spine
Field of view: 2.5 mm

CURRICULUM VITAE DR. ANNEGRET JANOVSKY

Work experience

Since January 2021	Product Marketing Manager Industrial Microscopy EMEA SSD, Olympus Europa SE & Co. KG (OEKG)
April 2017 – December 2020	Sales Specialist Industrial Microscopy, OLYMPUS Deutschland GmbH
June 2015 – March 2017	Territory Manager Manufacturing, Sales of all industrial product lines (NDT, RVI, ANI and Microscopy), OLYMPUS Deutschland GmbH
Mai 2002 – June 2015	Sales Microscopy in Material and Life Science, OLYMPUS Deutschland GmbH

Education

09/1997 – 08/1999	PhD studies at the University of Leipzig Graduation with the academic degree Dr.rer.nat in Mineralogy
09/1988 – 07/1993	Studies of Crystallography at the University of Leipzig Graduation as "Diplom-Kristallographin" Main focus on Mineralogy and Microscopy
Additional Skills/ Hobby	Microphotography: Grains of sand

Brandon river mouth, Ireland
Mineral sand
Field of view: 3 mm

Massa Carrara, Mediterranean Sea, Italy
Mineral sand
Field of view: 2.5 mm

Warnemünde,
Baltic Sea, Germany
Mineral sand, mainly quartz
Field of view: 3.1 mm

Hurghada, Red Sea, Egypt
Biogenic sand with forams
Field of view: 12.8 mm

Godafoss Waterfall, Iceland
Volcanic glass
Field of view: 1 mm

Playa del Verodal, El Hierro, Canary Islands, Spain
Volcanic mineral sand
Field of view: 8 mm

Whitefish Lake, Montana, USA
Mineral sand
Field of view: 8.1 mm

02 Portable X-Ray Fluorescence Spectroscopy Analysis of Agricultural Soils After the Gold King Mine Spill

G. Jha, S. Mukhopadhyay, *et al.*

ABSTRACT

In 2015, a million liters of heavy metal–contaminated water spilled into the Animas River from the Gold King Mine (Colorado, USA), attracting national attention about the water quality and agricultural production in the affected areas. In response to the concerns, surface soil elemental concentrations were analyzed in three New Mexico agricultural fields to determine potential threats to agronomic production. The irrigated fields were scanned using portable X-ray fluorescence (pXRF) spectrometry to monitor the spatiotemporal variability of lead (Pb), arsenic (As), copper (Cu), and chromium (Cr) before and after the growing season for 3 years. The geostatistical model with the lowest RMSE was chosen as the optimal model. The spatial dependence between the measured values exhibited strong to moderate autocorrelation for all metals except for As, for which spatial dependence was strong to weak. Some areas exceeded the soil screening limit of 7.07 mg As kg^{-1}. All sampling locations were below the screening limit at last sampling time in 2019. Mixed models used for temporal analysis showed a significant decrease only in As below the screening value at the end of the study. Results indicate that the agricultural soils were below the soil screening guideline values.

1 INTRODUCTION

On August 5, 2015, an inadvertent breach of the Gold King Mine (GKM) released ~11.3 million L of acid mine drainage into Cement Creek at the headwaters of the Animas River.[1] Approximately 2032 kg lead (Pb), 499 kg zinc (Zn), and 93 kg arsenic (As), among others, were released and flowed downstream.[2] The GKM is "one of an estimated 23000 abandoned mines dotting the state of Colorado".[3] The USEPA notes that "mining operations have greatly disturbed the land, adding to existing highly mineralized conditions in many areas that cause acidic conditions that release heavy metals to the surrounding environment".[3] They specifically note the prevalence of aluminum (Al), lead (Pb), zinc (Zn), cadmium (Cd), copper (Cu), iron (Fe), and manganese (Mn) as contributing polluters to surface water, subsurface water, surface soils, and stream sediments.

In northwestern New Mexico, alfalfa hay, pumpkin, watermelon, pepper, tomato, and other specialty crops are of strong economic importance. The irrigation water is delivered to farms through a series of community ditches or canals. At the time of the GKM spill, most farmers immediately closed their irrigation gates and ditches, allowing the most pollutant-laden water to pass down the river without entering their irrigation systems.

A substantive portion of the released metals were associated with suspended solids in the river. Sediments rich in Fe, Al, and other metals, however, were deposited as reddish orange sludge along the banks and throughout the river channel. A rapid assessment of the elemental concentration of riverbank sludge, irrigated croplands, and upland (non-irrigated) soils of the river valley affected and unaffected by the GKM was conducted.

In this assessment, Fe, Cu, Zn, As, and Pb increased in the order of control (non-irrigated) soils < irrigated soils < riverbank alluvium < riverbank sludge. Additionally, the riverbank sludge had concentrations of Pb ($n = 9$) that ranged from 509 to 859 mg kg^{-1}, all above the USEPA residential screening limit of 400 mg kg^{-1}. Therefore, a comprehensive monitoring plan was initiated out of concern that as hydrologic pulses occur, the metal-laden sludge deposited on the bottom of the river would become resuspended, enter the irrigation systems, and lead to an increase in toxic metal concentration in soils used for farming.

The deleterious effects of toxic metals to human health are well documented. Briefly, the main health effects associated with high levels of elements include nervous system disorders, liver and kidney failure and damage, anemia, cancer, cardiomyopathy, gastroenteritis, osteomalacia, brain damage, hematologic effects, hypertension, intestine tract distress, and tissue lesions, among others.[4]

Widespread concern exists as to the safety of produce if irrigated with potentially metal-laden water from the Animas River. The objective of this study was to perform a spatiotemporal analysis of elemental concentrations in agricultural soils of the Animas River watershed over a period of three cropping seasons (2017–2019) and compare monitored values to determine their potential threat to agronomic production. We hypothesized that the soil concentrations of several elements would increase over time in response to irrigation with water from the Animas River.

2 MATERIALS AND METHODS

2.1 General study area

The study was conducted on irrigated farm fields in San Juan County, NM. Geologically, the area is comprised of shale, sandstone, limestone, dolomite, and volcanic rock outcrops. Soils of the area are Alfisols, Aridisols, Entisols, and a few Mollisols. Soil temperature regime is dominantly mesic, with an aridic or ustic-aridic moisture regime.[5] The Koppen climate classification of the area is BSk (cold semiarid).[6] Soils feature carbonatic, mixed, or smectitic mineralogy. In this arid to semi-arid climate, almost all crops must be irrigated to produce sufficient yields. The soil series on the studied fields are described as Fruitland, Turley, and Garland.

2.2 Fieldwork

Three irrigated farm fields of 30, 17, and 8 ha were evaluated as part of this study. With the perimeter of each field, a random sampling scheme was established in ArcGIS (ESRI), which created a sampling density of ~3.2 points ha^{-1}. This resulted in a total of 175 points (two fields with 50 points each and one field with 75 points). The pre-determined sampling locations were downloaded into an eTrex (Garmin) handheld global positioning receiver for field geolocation. Elemental data collection was performed using a DP-6000 portable X-ray fluorescence (pXRF) spectrometer (Olympus®).

[7] Prior to operation, the instrument is checked with a stainless steel alloy, then operated on line power (110 VAC) using a portable power inverter at 15–40 keV. The instrument was operated in Soil Mode at 30 s per beam such that one complete scan was completed in 90 s. Validation of instrument performance was accomplished via National Institutes of Standards and Technology (NIST)-certified reference materials. The average recovery percentages were determined for all four sampling times during the study that did not vary by more than 15% from the actual certified values for the elemental concentrations.

The pXRF field sampling was conducted over 3 years. The Animas River watershed has only one growing season (from mid-April to mid-November). Portable XRF scans in November were considered to represent both post-growing conditions for the current season and pre-growing conditions for next growing season. Scanning was performed in an identical manner at the same sampling locations to allow for temporal analysis.

2.3 Statistical analysis

Descriptive statistics and correlation analysis of pXRF metal(loid) was analyzed in R studio (version 3.4.1). Pearson's correlation matrix was plotted using the *corrplot* function combined with the significance test ($p \leq .05$) in *Hmisc* package. Temporal changes in metal(loid) s were assessed in SAS version 9.4 using a design-based linear mixed model approach with sampling time as the fixed effect and random effects for field and the sampling time by field interaction. Additionally, a repeated statement fitted an unstructured covariance of the repeated measurements (the four sampling times) from the randomly chosen but repeatedly sampled locations within fields. When time was significant, pairwise comparisons among the four measurement times used model-based estimates and standard errors. Significance was set at $p \leq .05$. Temporal analysis of significant changes in metal(loid) concentrations were analyzed using SAS version 9.4.

2.4 Geostatistical analysis and spatiotemporal mapping

Spatiotemporal variability maps were interpolated for four metal(loid)s of concern using pXRF total concentrations sampling four times over a period of three growing seasons. Three different models were fit to total metal(loid) concentrations of As, Cr, Pb, and Cu. Root mean square error was considered as a measure of model performance, and the model with the lowest RMSE value was selected for each metalloid as the best fitted model for kriging interpolation[8]. Semivariogram parameters were interpreted to understand the insights of the fitted model. Sill is the variance on the dataset without knowing the spatial location, and nugget is the amount of variance that is not explained by the model as the distance between observations approaches zero (Allan, 2018). Nugget to sill ratios were interpreted to understand the strength of spatial dependence between sampling points. Semivariogram ranges were also interpreted as the range of spatial autocorrelation determining the strength of metal concentrations scanned using pXRF at one geographic location in the field relative to another scanning location separated by a distance. Spatial maps were interpolated using ordinary kriging in ArcGIS version 10.2.2 (ESRI) using the weighted averages of the known concentrations of metal(loid)s.

3 RESULTS AND DISCUSSION

3.1 Summary statistics

Total mean soil elemental concentrations were detected in the order Pb > Cu > Cr > As for each growing season. The Pb and Cu concentrations at all locations were below the soil screening levels of 400 and 3100 mg kg^{-1}, respectively. During the pre-growing 2017 season, the average total metal concentrations in the three fields were 50 mg kg–1 (Pb), 23 mg kg^{-1} (Cu), 17 mg kg^{-1} (Cr), and 8 mg kg^{-1} (As). In observing the maximum, median, and mean concentration values for As, at least one or more sampled locations exceeded the soil screening limit (SSL) value of 7.07 mg kg^{-1} recommended by the New Mexico Environment Department.[9] In total, 46.3% (number of locations exceeded/total number of scanning locations = 81/175) sampling locations exceeded the SSL for As during the 2017 pre-growing study period, and 43.4% (76/175) samples exceeded the SSL in the 2017 post-growing season. In the 2018 and 2019 post-growing seasons, the percentage of locations that exceeded the SSL values was reduced to 16.6% (29/175) and 7.4% (13/175), suggesting temporal decreases.

3.2 Correlation analysis between elements analyzed using pXRF

Several metals showed significant correlations with each other in the soil matrix. Combining the data from all three fields, Cu and Pb were positively correlated with significant correlation coefficient values ranging from .76 to .90 when metal concentrations pooled for all three fields were correlated and compared respective to the four sampling times.

These results were similar to the findings by other researchers using pXRF for multi-elemental analysis with strong correlations between Pb and Cu.[10, 11] Cu and Cr, Pb and Cr, As and Cr, and As and Cu showed weak or moderate correlations with each other or sometimes negative correlations. Additional works in the Animas River watershed after the GKM spill established that there was an association between Pb, Cu, and Zn and Fe-minerals such as jarosite, goethite, and clays in sediment.[12]

3.3 Spatiotemporal variability of metals in agricultural fields

Figures 1–4 depict the spatial distribution of the four metal(loid)s of interest interpolated over the four sampling dates. There were some hotspots of As in the fields until the third sampling date. All soil As concentrations were below the SSL of 7.07 mg kg^{-1} and therefore were considered below the risk assessment guidelines during the last sampling date in the 2019 post-growing season (**Figure 1**).

Cr concentration increased in the soil collected during the last sampling time for all three fields (**Figure 2**). This increase was more noticeable in fields 1K and 3K, which were under pivot irrigation. Field 2S, which was under furrow irrigation, had an increase in Cr at some locations. Regions of higher Pb concentration also showed high Cu concentration. However, Cu (**Figure 4**) does not show much variability after any irrigation season. Lead and Cu show similar adsorption behavior and tend to coexist in soil,13 however, lead tends to become less soluble with increasing pH of soil solution as more calcium carbonate is added through irrigation

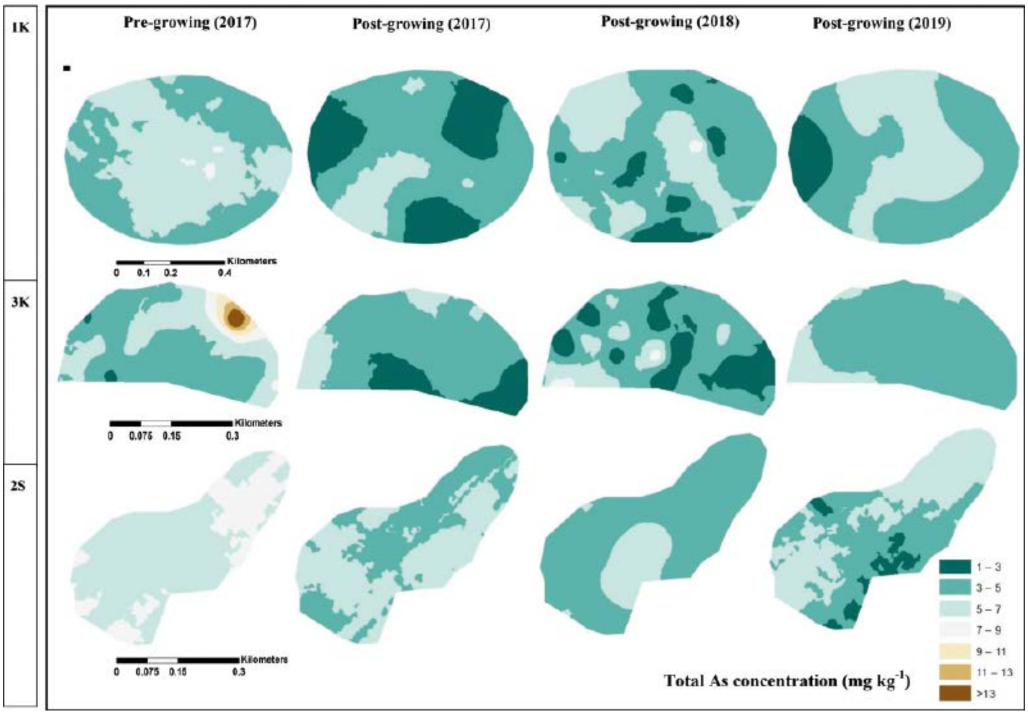

Figure 1: Spatial variability interpolation maps of total As concentration in three agricultural fields under irrigated conditions for four sampling dates from 2017 to 2019.

water. River water was collected near the inlet irrigation gates for three growing seasons and analyzed for all metal concentrations, showing values below the USEPA screening levels.

Samples located closer to each other by distances less than the range are spatially correlated and contribute to kriging predictions.[14] The nugget to sill ratios for As were moderate for fields 1K and 2S. The nugget to sill ratio for field 3K was moderate for pre- and post-growing 2017 and strong for post-growing 2018 but was weak for post-growing 2019. Nugget to sill ratios for Cr, Pb, and Cu were moderate to strong.

Weak spatial dependence of As is due to variability at scales smaller than the two closest sampling points in any one field. The inability to capture small-scale variability for As in this study was also due to the increasing number of nondetectable As readings using the pXRF. The nugget to sill ratio for Cr, Cu, and Pb showed strong to moderate spatial dependence during all four sampling times for all three fields. The spatial dependence estimated using semivariogram parameters are predictions at unsampled locations in the field based on the known values from sampled locations.

Maps based on kriging predictions can be used for future study by sampling locations less than the range in fields. In furrow-irrigated fields, it is important to understand that redox conditions might be different in the top of ridges and bottom of furrows. In this study, samples were scanned from random locations with a mix of both ridge and furrows without any biased separation. Therefore, it is important to sample both locations in furrow-irrigated systems to get a proper representation of elemental concentration in future studies.

3.4 Temporal analysis

At the time of the GKM spill it was hypothesized that there would be a surge in metal concentrations in agricultural field soils as irrigation resumed once the irrigation ban was lifted. There was a significant increase in total Cr concentration at the end of three growing seasons. We also measured a significant decrease

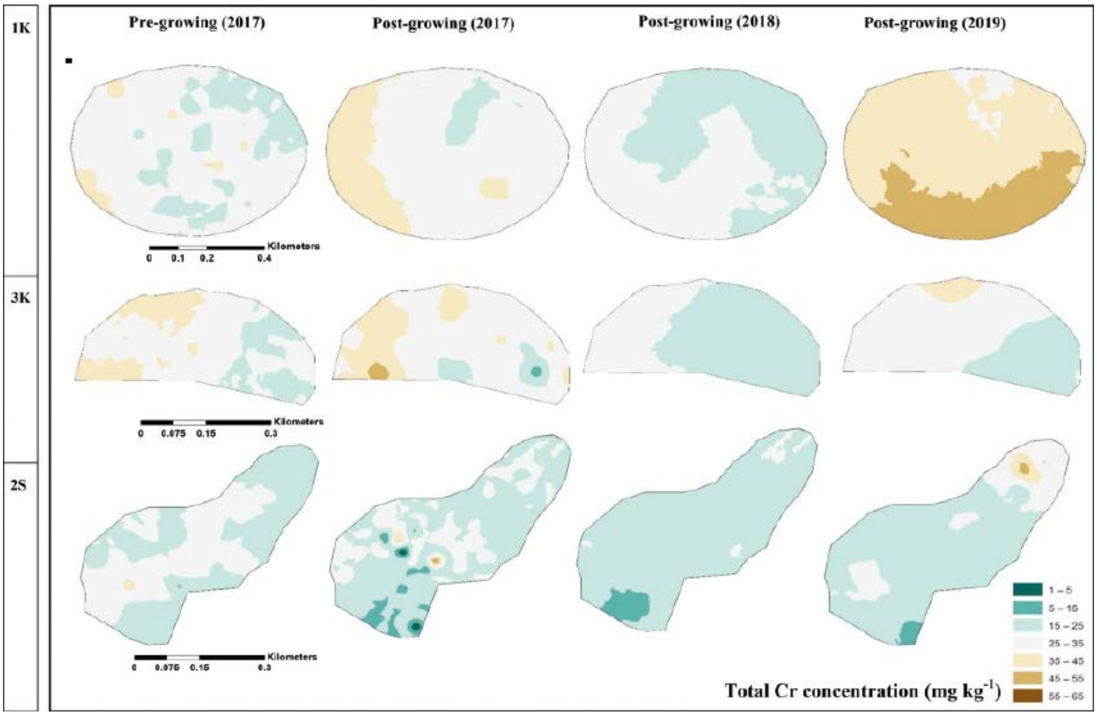

Figure 2: Spatial variability interpolation maps of total Cr concentration in three agricultural fields under irrigated conditions for four sampling dates from 2017 to 2019.

in total As and Pb at the third sampling date in post-growing 2018 (**Figures 1** and **2**).

Contrary to the hypothesis of this study, As decreased 2.3 ± 0.3 mg kg^{-1} from March 2017 to November 2019. The estimated As (5.3 ± 0.2 mg kg^{-1}) after three growing seasons decreased to below the soil screening level. However, there was a significant increase (9.4 ± 1.3 mg kg^{-1}) in mean Cr concentration. This study did not analyze the oxidation state of Cr and focused only on total concentration. It is recommended for future studies to look into Cr speciation and how it interacts with soil matrix and plants. Decreases in average Cu concentrations (1.7 ± 0.9 mg kg^{-1}) were not significant, whereas decreases in mean Pb concentration (1.0 ± 2.9 mg kg^{-1}) were significant between March 2017 and November 2018 but not between March 2017 and November 2019. Both Cu and Pb were below the soil screening level for all fields sampled at all sampling times.

4 CONCLUSIONS

This study evaluated agricultural fields in the Animas River watershed, NM, for four potential metal(loid) contaminants of concern (Pb, As, Cu, Cr) following the GKM spill of 2015. Portable X-ray fluorescence was used to determine metal(loid)s at a total of 175 sampling locations spread across three fields over 3 yr. Geostatistical models were fit to each metal(loid) for each agricultural field for each sampling date. Spatial interpolation was used to infer spatial variation, and mixed models were used to infer the temporal variation in metal(loid) concentrations. Spatial interpolation revealed an overall decrease in surface soil As concentration between 2017 and 2019. However, there were some areas in the fields where As concentrations still exceeded the regional soil screening limits of 7.07 mg kg^{-1} for the first three sampling times. Arsenic concentration in soils decreased to significantly below the soil screening value (7.07 mg kg^{-1}) by the end of 2019 growing season for all fields. We found

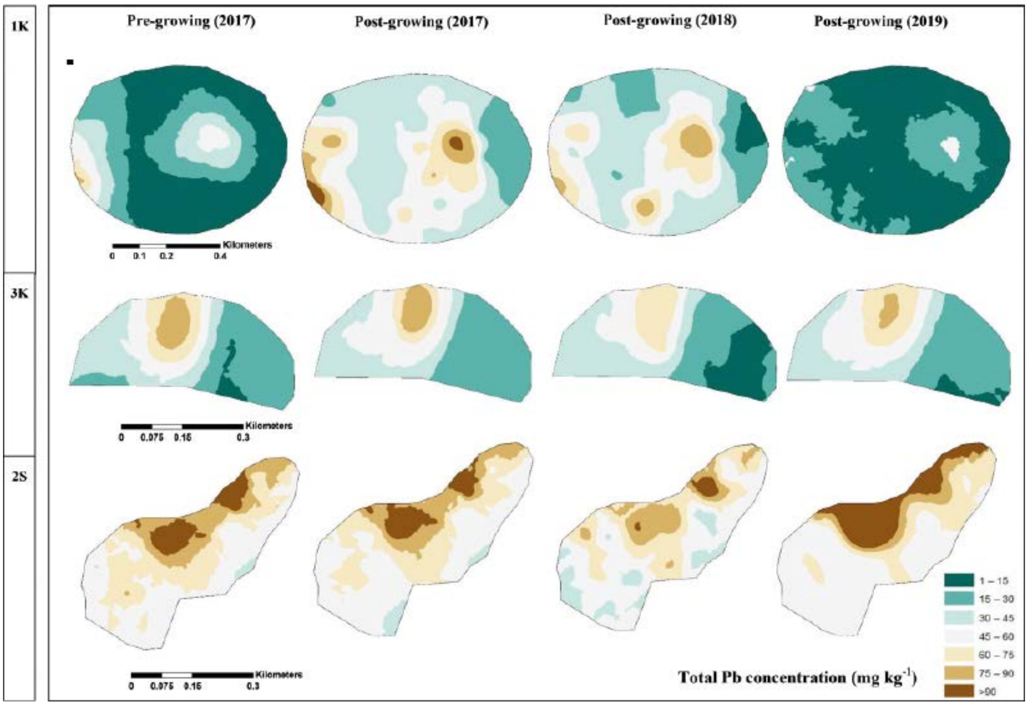

Figure 3: Spatial variability interpolation maps of total Pb concentration in three agricultural fields under irrigated conditions for four sampling dates from 2017 to 2019.

that all three fields were below the risk assessment guidelines. This study is important in environmental monitoring of agricultural soils after the GKM spill of 2015 to help farmers and consumers make informed decisions of the field soils used for growing important crops like alfalfa, corn, and pumpkin in northwestern New Mexico.

REFERENCES

[1] *New Mexico Environment Department (NMED). (2015). Gold King Mine wastewater spill of Wednesday, August 5, 2015: Timeline and archive updates. https://www.env.nm.gov/animas-river-timeline.*

[2] *Chief, K., Artiola, J. F., Wilkinson, S. T., Beamer, P., & Maier, R. M. (2015). Understanding the Gold King Mine spill (Fact Sheet). University of Arizona.*

[3] *USEPA. (2015). Gold King Mine - watershed fact sheet. https:// www.epa.gov/sites/production/files/2015-08/documents/ goldkingminewatershed-factsheetbackground.pdf.*

[4] *Brevik, E. C., & Burgess, L. C. (2013). Soils and human health. CRC Press.*

[5] *Soil Survey Staff. (2006). Land resource regions and major land resource areas of the United States, the Caribbean, and the Pacific Basin. https://www.nrcs.usda.gov/wps/portal/nrcs/detail/soils/ survey/?cid=nrcs142p2_053624.*

[6] *Kottek, M., Grieser, J., Beck, C., Rudolf, B., & Rubel, F. (2006). World map of the Köppen-Geiger climate classification updated. Meteorologische Zeitschrift, 15(3), 259–263. https://doi.org/10.1127/0941- 2948/2006/0130.*

[7] *Weindorf, D. C., & Chakraborty, S. (2016). Portable X-ray fluorescence spectrometry analysis of soils. Soil Science Society of America Journal, 84(5), 1384–1392. https://doi.org/10.1002/saj2.20151.*

[8] *Ritter, A., & Muñoz-Carpena, R. (2013). Performance evaluation of hydrological models: Statistical significance for reducing subjectivity in goodness-of-fit assessments. Journal of Hydrology, 480, 33–45. https://doi.org/10.1016/j.jhydrol.2012.12.004.*

[9] *New Mexico Environment Department (NMED). (2017). Risk assessment guidance for site investigations and remediation. Volume I: Soil screening guidance for human health risk assessments. https://www.env.nm.gov/wp-content/uploads/sites/12/2016/11/ Final-NMED.*

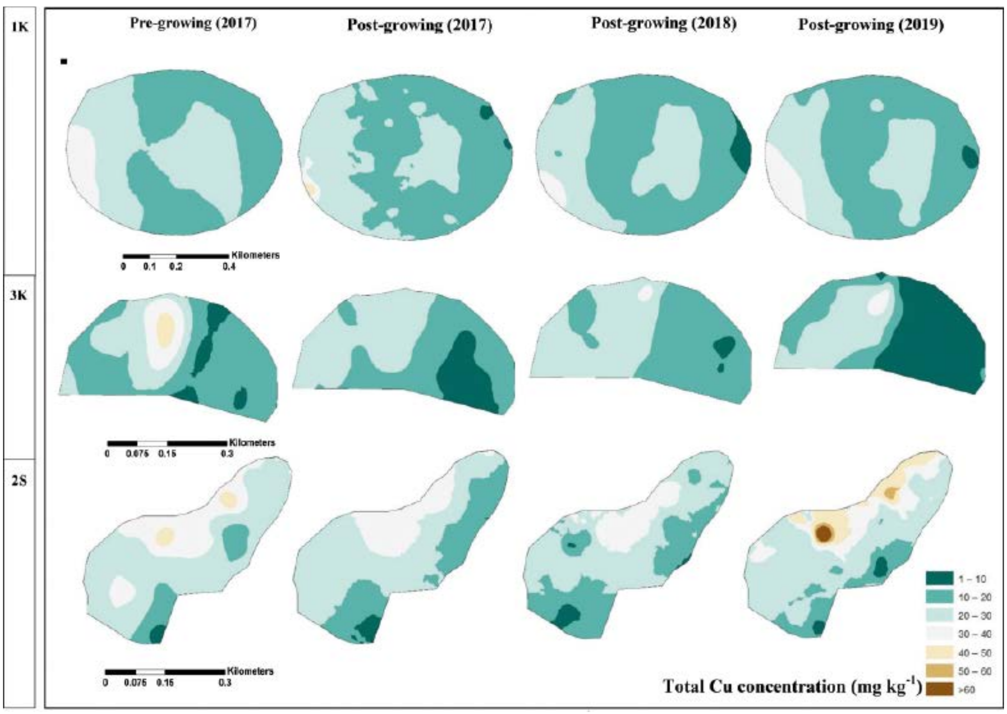

Figure 4: Spatial variability interpolation maps of total Cu concentration in three agricultural fields under irrigated conditions for four sampling dates from 2017 to 2019.

[10] *Chakraborty, S., Man, T., Paulette, L., Deb, S., Li, B., Weindorf, D. C., & Frazier, M. (2017). Rapid assessment of smelter/mining soil contamination via portable X-ray fluorescence spectrometry and indicator kriging. Geoderma, 306, 108–119. https://doi.o.*

[11] *Paulette, L., Man, T.,Weindorf, D. C.,&Person, T. (2015). Rapid assessment of soil and contaminant variability via portable X-ray fluorescence spectroscopy: Copşa Mică, Romania. Geoderma, 243, 130–140. https://doi.org/10.1016/j.geoderma.2014.12.025.*

[12] *Rodriguez-Freire, L., Avasarala, S., Ali, A. M. S., Agnew, D., Hoover, J. H., Artyushkova, K., Latta, D. E., Peterson, E. J., Lewis, J., Crossey, L. J., Brearley,A. J., Cerrato, J.M.,&Brearley,A. J. (2016). Post-Gold King Mine spill investigation of metal .*

[13] *Sharma, P., & Dubey, R. S. (2005). Lead toxicity in plants. Brazilian Journal of Plant Physiology,.*

[14] *Cambardella, C. A., Moorman, T. B., Novak, J. M., Parkin, T. B., Karlen, D. L., Turco, R. F., & Konopka, A. E. (1994). Field-scale variability of soil properties in central Iowa soils. Soil Science Society of America Journal, 58(5), 1501–1511. https://doi.*